Temporal and spatial analysis of meteorological drought characteristics in the upper Blue Nile river region

Mosaad Khadr

ABSTRACT

Drought is a costly natural hazard affecting socio-economic activity and agricultural livelihoods, as well as adversely impacting public health and threatening the sustainability of many natural environments. This study was carried out to characterize the temporal and spatial characteristics of meteorological drought in the upper Blue Nile basin to provide a framework for sustainable water resources management. Analysis of historical droughts was undertaken by converting observed monthly precipitation records (1960–2008), for 22 meteorological stations, to the standardized precipitation index (SPI). The SPI was computed at multiple time steps and the Mann–Kendall test was applied on monthly SPI time series for trend detection, and finally severity areal extent frequency (SAF) curves were developed to assess the recurrence pattern of drought severity. Several drought events were observed during the long rainy season and also the short rainy season, and the drought extent and influence were very severe in 1965 and the 1980s. Trend analysis showed statistically insignificant trends in SPI time series, and SAF curves indicated that droughts with a short return period and high degree will cover only small areas of the basin, while only a near-normal drought with a long return period may spread over the whole region.

Key words | Blue Nile river, meteorological drought, standardized precipitation index

Mosaad Khadr
Faculty of Engineering,
Tanta University,
Tanta 31111,
Egypt
E-mail: *mosaad.khadr@f-eng.tanta.edu.eg*

INTRODUCTION

Drought is one of the most damaging climate-related hazards, and has been a major concern of mankind for centuries (Sivakumar *et al.* 2005; IPCC 2012). It can affect large areas and may have serious impacts which depend on the severity, duration, and spatial extent of the precipitation deficit (European Commission 2007). Drought impacts are non-structural and spread over a larger geographical area than the damages that result from other natural hazards (Belayneh 2012). Quantifying the impacts and providing disaster relief are far more difficult tasks for drought than for other natural hazards since these impacts can filter through environmentally, socially and economically for months, years and even decades (Wilhite 2005; Bordi & Sutera 2007; Edossa *et al.* 2010). It is difficult to determine the onset and end of drought, therefore scientists and policy makers often disagree on the basis for declaring an end to drought (Tiwari *et al.* 2007; Wilhite *et al.* 2014). Different types of drought are identified in a practical sense, as drought differs between regions and its impacts vary significantly because of differences in economic, social, and environmental characteristics (Svoboda 2000; WMO 2006). All types of drought originate from a deficiency of precipitation, although other factors such as high winds, high temperatures, and low relative humidity may exacerbate the drought's severity (Mishra & Singh 2010). The main purpose of any drought monitoring system is to identify various drought indices to provide information to resources managers and system operators (Keyantash & Dracup 2002; Valipour 2012). Several drought indices are used in drought assessment and monitoring based on rainfall data (NDMC 2006; Hayes 2013; Wilhite *et al.* 2014). The most commonly used drought indices as reported in Wilhite (2005) and Valipour (2013a, 2013b) are

doi: 10.2166/nh.2016.194

the Palmer drought severity index (PDSI) (Palmer 1965), crop moisture index, standardized precipitation index (SPI) (McKee *et al.* 1993) and surface water supply index (Shafer & Dezman 1982). In this study, drought vulnerability in the upper Blue Nile river basin was investigated using the SPI, a meteorological index developed by McKee *et al.* (1993). The advantage of this index is that it identifies emerging drought months sooner than the PDSI, and can be computed at various timescales (NDMC 2006). This study aimed to address multi-nature aspects of drought with its several features; the frequency of drought occurrence and its spatial distribution to identify drought-prone areas; and drought vulnerability at multiple time steps, such as 3, 6, 9, 12, and 24 months. The severity and the frequency of the monthly drought periods were analyzed next and finally, the areal extent, the cumulative severity and the duration of common drought periods were examined. To the best of our knowledge, the issue of water resources management in the context of drought so far has not been addressed in the eastern Nile basin in general as well as in Egypt in particular. Results presented in this paper are part of an ongoing effort to develop a new integrated framework for water resources management in the context of drought. Our approach consists of the integration of qualitative modeling for drought monitoring, drought forecasting (Khadr 2015), a drought management plan, and a simulation model for the operation of the Aswan High dam in Egypt (Khadr & Schlenkhoff 2014). It is hoped that the proposed approach and our findings obtained in this study are useful for further research in the area of water resources management.

METHOD AND MATERIALS

Study region and data set

The Ethiopian highlands generate a discharge of 87% of the total Nile flow at the Aswan High dam in Egypt (Woodward *et al.* 2007; Zaroug *et al.* 2014). The Blue Nile originates from Lake Tana in the Ethiopian Highlands, at elevations of 2,000–3,000 m, and contributes about 60–69% of the main Nile discharge (Abu-Zeid & Biswas 1996; Conway 2005). The part of the watershed of the Blue Nile river basin which is under the Ethiopian territory is named the upper Blue Nile river basin (UBNRB). The UBNRB study area is located in the western part of Ethiopia, between 7° 45′ and 12° 45′N and 34° 05′ and 39° 45′E, and comprises 17% of the area of Ethiopia (176,000 km^2 out of 1,100,000 km^2). Figure 1 shows that the altitude of the UBNRB ranges from 511 to 4,052 m and the Blue Nile and its tributaries have a general slope towards the northwest, however the slopes are steeper in the east than in the west and northeast areas of the UBNRB. The average annual flow of the Blue Nile at the Sudan-Ethiopian border is about 48,660 million m^3, which represents more than 40% of Ethiopia's total surface water resources (Conway 2000). Hence, the UBNRB represents a substantial water resource for Ethiopia and also for the downstream countries of Sudan and Egypt.

Forty-nine years (January 1960–December 2008) of daily precipitation data from 22 meteorological stations in the upper Blue Nile basin were used in this study to analyze drought events. The selected stations represent a good spatial coverage across the study region (Figure 1). The average precipitation over the Blue Nile is 1,394 mm and is higher than the other sub-basin of the Nile basin

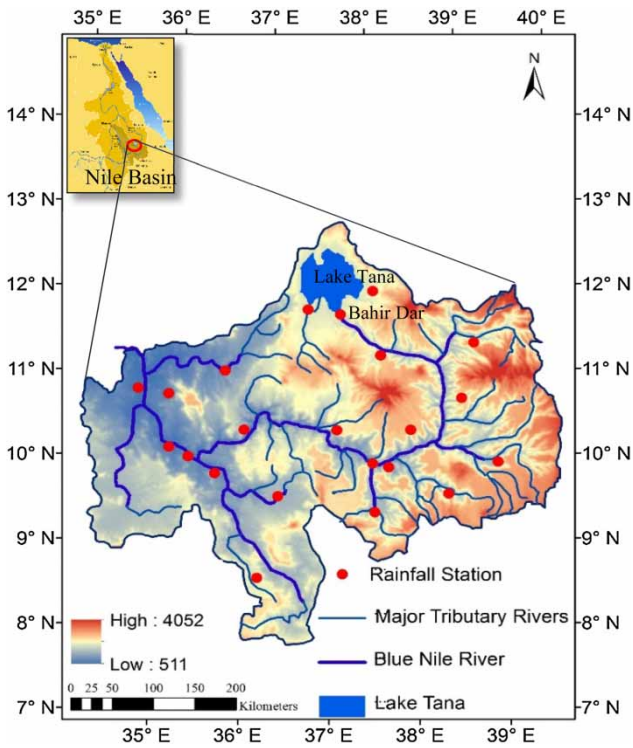

Figure 1 | Digital elevation model (DEM) of the UBNRB with locations of meteorological stations.

(Nour-El-Din 2013). The minimum and maximum values of the mean annual rainfall over the UBNRB, within the studied period, are 1,464 and 1,054 with an overall average of 1,260 mm as shown in Figure 2. Locally, the climatic seasons are defined as: the dry season (Bega) from October to the end of February; the short rain period (Belg) from March to May; and the long rainy period (Kiremt) from June to September, with the greatest rainfall occurring in July and August. The rainfall distribution is highly variable both spatially – decreasing from the southwest to the east and northeast – and temporally, i.e. over the yearly seasons. Figure 3 shows the mean monthly precipitation, and the corresponding standard deviation, for the Bahir Dar station on the southern shore of Lake Tana. About 80% of the annual precipitation is received during the period of June to September. The standard deviation ranges between 14% of the mean in wet months and 42% of the mean in dry months, which indicates inter-annual variability of the monthly precipitation (Figure 3).

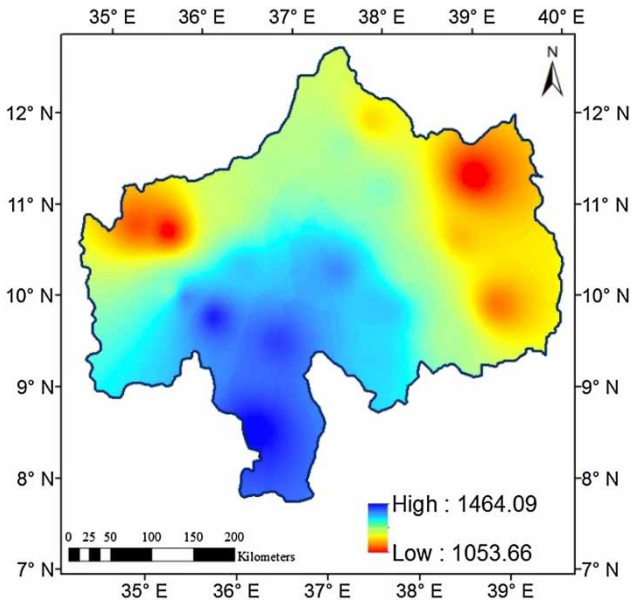

Figure 2 | Mean annual precipitation (mm) over the upper Blue Nile river (1960–2008).

Methodology

The methodology presented in this paper and applied to UBNRB consisted of calculation of the SPI values for multiple timescales, analysis of the temporal characteristics, the spatial interpolation of SPI gauge data, the generation of gridded SPI data, and trend analysis of SPI time series, followed by the analysis of spatial characteristics of droughts in the UBNRB for monthly and mean annual droughts and multiple timescales.

The SPI

The SPI was chosen for this study because of its simplicity and being based solely on the accessible precipitation data. The SPI is based on an equi-probability transformation of aggregated monthly precipitation into a standard normal variable (McKee *et al.* 1993), and is recommended by the World Meteorological Organization as a standard to characterize meteorological droughts (Dutra *et al.* 2013). McKee *et al.* (1993) assumed an aggregated precipitation Gamma distributed, and used a maximum likelihood method to

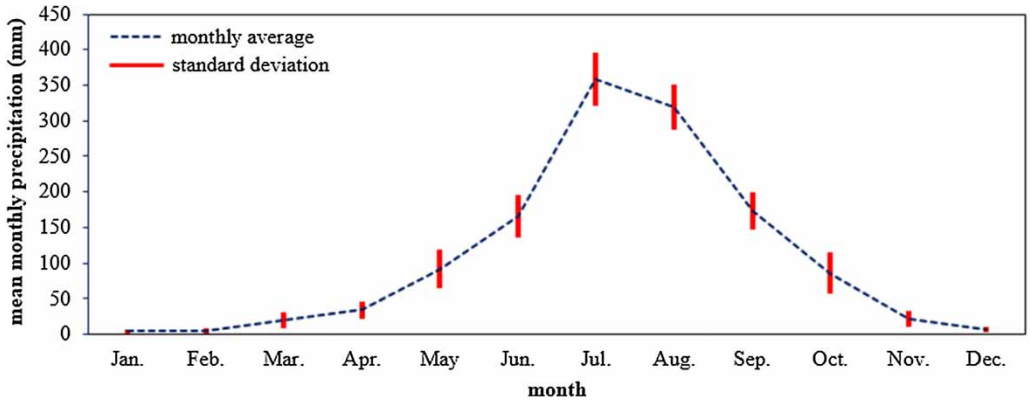

Figure 3 | The monthly average precipitation along with the corresponding standard deviation for Bahir-Dar station.

estimate the parameters of the distribution. In most cases, the Gamma distribution is the distribution that best models observed precipitation data. The density probability function for the Gamma distribution is given by the expression (Cacciamani *et al.* 2007):

$$g(x) = \frac{1}{\beta^{\alpha}\Gamma(\alpha)} x^{\alpha-1} e^{\frac{-x}{\beta}}, \text{ for } x > 0 \quad (1)$$

where $\alpha > 0$ is a shape parameter, $\beta > 0$ is a scale parameter and $x > 0$ is the precipitation amount. $\Gamma(\alpha)$ is the Gamma function and defined by:

$$\Gamma(\alpha) = \int_0^{\infty} x^{\alpha-1} e^{-x} dx \quad (2)$$

Computation of the SPI involves the fitting of a Gamma probability density function to a given frequency distribution of precipitation totals for a station. The alpha and beta parameters of the Gamma probability density function are estimated for each station, for each timescale of interest (1, 3, 12, 48 months, etc.) and for each month of the year. After estimating the alpha and beta coefficients the density of probability function $g(x)$ is integrated with respect to x and we obtain an expression for cumulative probability $G(x)$ that a certain amount of rain has been observed for a given month and for a specific timescale:

$$G(x) = \int_0^{x} g(x)dx = \frac{1}{\beta^{\alpha}\Gamma(\alpha)} \int_0^{x} x^{\alpha-1} e^{\frac{-x}{\beta}} dx \quad (3)$$

The Gamma function is not defined by $x = 0$, and since there may be no precipitation the cumulative probability becomes:

$$H(x) = q + (1-q)G(x) \quad (4)$$

where q is the probability of no precipitation. The cumulative probability is then transformed into a normal standardized distribution with null average and unit variance, from which we obtain the SPI (Khadr *et al.* 2009). The SPI is then defined as:

$$SPI = -\left(t - \frac{c_0 + c_1 t + c_2 t^2}{1 + d_1 t + d_2 t^2 + d_3 t^3}\right) \text{ for } 0 < H(x) < 0.5 \quad (5)$$

$$SPI = +\left(t - \frac{c_0 + c_1 t + c_2 t^2}{1 + d_1 t + d_2 t^2 + d_3 t^3}\right) \text{ for } 0.5 < H(x) < 1 \quad (6)$$

where

$$t = \sqrt{\ln\left[\frac{1}{(H(x))^2}\right]} \text{ for } 0 < H(x) < 0.5 \quad (7)$$

$$t = \sqrt{\ln\left[\frac{1}{(1-H(x))^2}\right]} \text{ for } 0.5 < H(x) < 1 \quad (8)$$

where c_0, c_1, c_2, d_1, d_2 and d_3 are constants with the following values:

$$c_0 = 2.515517 \quad c_1 = 0.802853 \quad c_2 = 0.010328$$
$$d_1 = 1.432788 \quad d_2 = 0.189269 \quad d_3 = 0.001308$$

Drought intensity classification in various categories with different values of SPI is given in Table 1. Positive SPI values indicate greater than median precipitation, and negative values indicate less than median precipitation. In this study, the SPI program developed by the author (Khadr 2011) is used to compute the time series of drought indices (SPI) for each station in the basin and for each month of the year at different timescales (3, 6, 9, 12 and 24 months).

Mann-Kendall trend test

The nonparametric Mann–Kendall (MK) test, also known as Kendall's τ au test or the MK trend test, is widely used to

Table 1 | Weather classification based on the SPI

SPI	Classification
>2	Extremely wet
1.5 to 1.99	Very wet
1 to 1.49	Moderately wet
0.99 to –0.99	Near normal
–1 to –1.49	Moderately dry
1.5 to –1.99	Severely dry
–2 and less	Extremely dry

evaluate trends in hydrological time series (Yue *et al.* 2002; Blain 2012). The MK test was applied to all SPI time series to examine the trends in the SPI data series. The MK test is based on the test statistic S defined as follows:

$$S = \sum_{i=1}^{n-1} \sum_{j=i+1}^{n} \mathrm{sgn}(y_i - y_j) \tag{9}$$

where y_j are the sequential data values, n is the length of the data set and

$$\mathrm{sgn}(y_i - y_j) = \begin{cases} 1 & if\ (y_i - y_j) > 0 \\ 0 & if\ (y_i - y_j) = 0 \\ -1 & if\ (y_i - y_j) < 0 \end{cases} \tag{10}$$

Mann (1945) and Kendall (1975) documented that when $n \geq 8$, the statistic S is approximately normally distributed with the mean and the variance as follows:

$$E(S) = 0 \tag{11}$$

$$V(S) = \frac{n(n-1)(2n+5) - \sum_{p=1}^{u} t_p(t_p-1)(2t_p+5)}{18} \tag{12}$$

where n = number of data, t_p = the number of ties for the pth value (number of data in the pth group), u = the number of tied values (number of groups with equal values/ties).

The standardized MK test statistic Z_{MK} is computed by:

$$Z_{MK} = \begin{cases} \dfrac{S-1}{\sqrt{Var(s)}} & S > 0 \\ 0 & S = 0 \\ \dfrac{S+1}{\sqrt{Var(s)}} & S < 0 \end{cases} \tag{13}$$

The standardized MK statistic Z follows the standard normal distribution with mean of zero and variance of one. The hypothesis that there is no trend will be rejected if:

$$|Z_{MK}| > Z_{1-\alpha/2} \tag{14}$$

$Z_{1-\alpha/2}$ is the value read from a standard normal distribution table, with α being the significance level of the test. At the 99% significance level, the null hypothesis of no trend is rejected if $|Z_{MK}| > 2.575$; at the 95% significance level, the null hypothesis of no trend is rejected if $|Z_{MK}| > 1.96$; and at 90% significance level, the null hypothesis of no trend is rejected if $|Z_{MK}| > 1.645$.

Temporal and spatial analysis of drought in UBNRB

The temporal and spatial characteristics of drought in UBNRB were assessed by analyzing the SPI values. Firstly, the temporal variation of SPI was assessed based on the SPI characteristics presented in Table 1, using the calculated SPI from the time series of the monthly precipitation. The magnitude of a considered drought event (DM), which is the summation of negative SPI values, was also calculated at all stations. Secondly, the computed SPI values based on various timescales within the study period (January 1960–December 2008) were entered into a geographical information system (GIS) database. Then, the spatial characteristics of drought during these severe dry periods were analyzed and visualized within the GIS. The spatial distribution of the SPI was determined through spatial interpolation techniques, using the inverse distance weighting (IDW) method to analyze the meteorological drought with due emphasis to ungauged catchments. The IDW, which is a deterministic method for multivariate interpolation, relies on the theory that the unknown value of a point is more influenced by closer points than by points further away (Khadr & Schlenkhoff 2014a). The SPI characteristics presented in Table 1 were used to generate drought maps for the UBNRB using GIS.

Drought severity areal extent frequency (SAF) curves were developed for the UBNRB using the computed gridded monthly SPI values for various timescales. The probability of annual drought occurrence for each year and in each grid was estimated by dividing the number of months that have a negative SPI value for the particular timescale by 12, then the annual weighted cumulative drought severity in each grid was estimated by multiplying the annual sum of the negative SPI values for a particular timescale by the probability of drought occurrence for each year. The map produced in the GIS was then used to obtain the drought severity associated with the areal extent and to perform frequency analysis for each drought areal extent percentage to

associate the drought severity with return periods, considering an adequate probability distribution. In the end, the families of SAF curves corresponding to different return periods were constructed by plotting area (in percent of whole region) versus average SPI in each category.

RESULTS AND DISCUSSION

Temporal characteristics of the drought in UBNRB

Daily precipitation records were converted to monthly values after the homogeneity of data was checked using the von Neumann ratio, standard normal homogeneity test and the Range test (Peterson *et al.* 1998; Karabork *et al.* 2007; Khadr 2011). The data sets of all the stations considered in this study were found to be homogeneous. On the basis of monthly precipitation of 49 years covering 1960–2008, 22 series of SPI for the UBNRB were calculated for multiple timescales, using the monthly precipitation. Analysis of the computed SPI time series revealed the most severe and extreme droughts occurred in the study area. Since it is virtually impossible to illustrate all results for all stations, we therefore primarily use the results from the Bahir Dar station, which is situated on the southern shore of Lake Tana (Figure 4). Since the SPI in a 1-month timescale fluctuates rapidly between positive and negative values, detection of the start and end of a drought event is unreliable. Therefore, in this paper the SPI with 3-, 6-, 9-, 12-, and 24-month timescales were used to identify drought events. Figure 4 describes the changes in drought characteristics in frequency (time/month), duration (month) and magnitude of SPI for Bahir Dar station. Figure 4 represents SPI values for four different timescales, namely 3, 6, 9 and 12 months.

As one can see in Figure 4, a drought's characteristics change with time and at longer timescales droughts become less frequent but their duration increases. The time series of 3-month SPI (Figure 4(a)) shows that the station experienced frequent moderate, severe and extreme droughts. Analysis of the relative frequency of occurrence (Table 2) of the annual minimum monthly SPI, during rainy seasons as mentioned earlier, shows that May is the month during which the 3-month SPI most frequently takes the annual minimum value (13.7%), and it is followed by July (8.22%). The annual minimum SPI values for the 6-, 9-, 12-, and 24-month time series for the period of analysis were mainly observed in June, May, August and June, respectively (Table 2).

Three-month SPI time series show extreme droughts in 1961, 1965, 1980, 1982, 1984, 1990, 1996, 1999, and 2002. The 1982, 1990 and 1999 droughts were very extreme and had a substantial impact, especially on downstream countries (Figure 4(a)). Visual inspection of 6-, 9-, and 12-month SPI time series indicated that drought was quite frequent during the study period. Results show that for Bahir Dar station, the maximum negative SPI values for 3-, 6-, 9-, 12-, and 24-month timescales were –2.69, –2.71, –2.77, –2.54 and –2.12, and these values were found in the years 1990, 1991, 1990, 1983 and 1983, respectively (Figure 4(a)–4(e)). Between June 1981 and April 1987, Bahir Dar station was affected by the longest duration of drought event, which reached a minimum value of –2.54 in April 1983 according to SPI12 series. Figure 4 also shows that the main dry periods are identified clearly using timescales larger than 6 months (9, 12 and 24 months). As seen in Figure 5, the mean annual drought magnitude of each year for the study area indicates that several significant droughts were identified within the study period, such as the years 1965, 1982, 1983, 1984, 1990 and 1992; however, the longest droughts occurred during the 1980s.

Trend analysis was performed using the MK test of the null hypothesis of trend absence in the SPI time series, against the alternative of trend. The result of the test is returned in $h_m = 0$, for all SPI series, and indicates a failure to reject the null hypothesis at the 90% significance level. Moreover, Table 3 indicates a failure to reject the null hypothesis at the 90% significance level since $|Z_{MK}| < 1.645$ for SPI3, SPI6, SPI9, SPI12 and SPI24, which means that all investigated trends are statistically insignificant.

Spatial characteristics of drought in UBNRB

The spatial analysis was performed using the gridded SPI values estimated for various timescales and for each month of the year. Based on the SPI characteristics presented previously in Table 1, drought maps were generated for the UBNRB basin using IDW methodology for

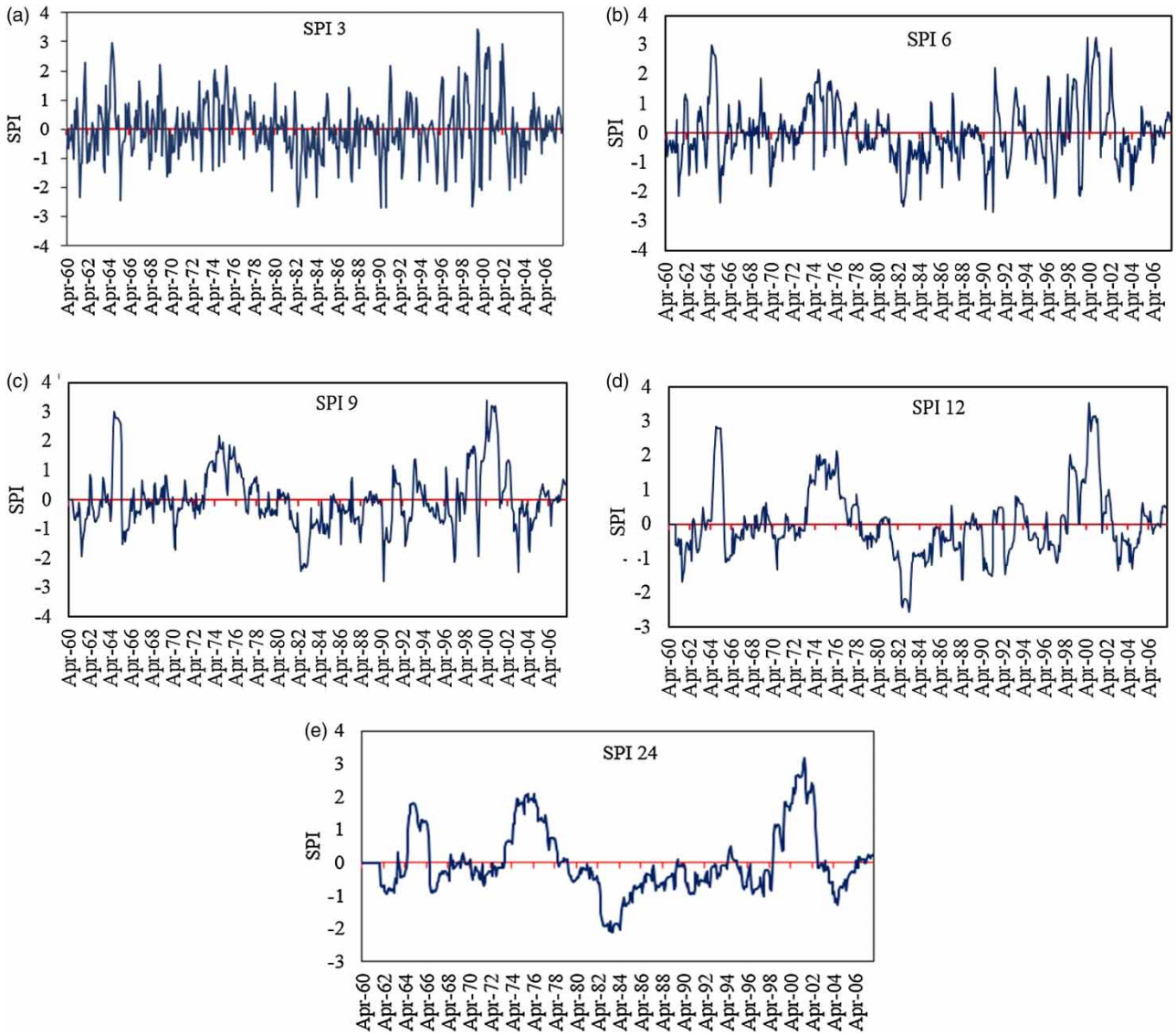

Figure 4 | SPI time series based on the total monthly precipitation at Bahir Dar station (1960–2008). (a) SPI3, (b) SPI6, (c) SPI9, (d) SPI12, (e) SPI124.

interpolation. Two recognizable severe dry periods were revealed, considering only the annual minimum spatial SPI value. The first period occurred during the year 1965 and is characterized as an extreme drought event. The second period was during the 1980s and reached its maximum value in 1984. The drought period during 1980 is characterized as a severe drought for the whole area of UBNRB. Maps which are shown in Figure 6(a)–6(d) show several extreme drought events for the months June 1965 and August 1984, respectively, using different SPI timescales. For the year 1965, both SPI3 and SPI6 show that the area in the center of the study area and with a direction north to east and southeast was the area affected most by the drought, which is in accordance with Dorosh & Rashid 2013; Masih *et al.* 2014). However, for the year 1984, both SPI3 and SPI6 show that the pattern changed and indicate that the most drought affected areas were the eastern, western and northern areas of the region. The spatial distribution of a particular annual drought episode was assessed using the estimated cumulative SPI. Figure 7(a)–7(f) show the spatial variation of the annual cumulative 3-month SPI and the annual 6-month SPI, respectively, for 1965, 1982

Table 2 | Relative frequency of occurrence (%) of annual minimum monthly SPI for various timescales using SPI at Bahir Dar station

Month	SPI 3	SPI 6	SPI 9	SPI 12	SPI 24
January	9.59	7.35	4.84	6.67	7.50
February	0.00	8.82	6.45	5.00	7.50
March	10.96	10.29	9.68	3.33	7.50
April	9.59	7.35	6.45	6.67	5.00
May	13.70	10.29	12.90	8.33	7.50
June	6.85	11.76	9.68	13.33	12.50
July	8.22	8.82	9.68	10.00	10.00
August	6.85	10.29	11.29	13.33	10.00
September	6.85	5.88	6.45	10.00	10.00
October	6.85	5.88	8.06	6.67	7.50
November	6.85	5.88	6.45	8.33	7.50
December	13.70	7.35	8.06	8.33	7.50

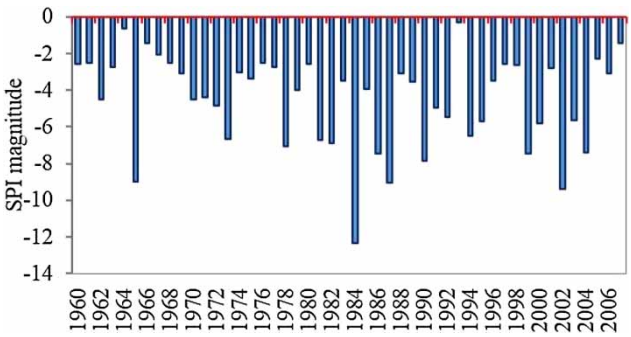

Figure 5 | Mean annual drought magnitude of the negative SPI values for the study area.

and 1984, which were the driest years in the investigated record. As seen, during the year 1965 the annual cumulative drought intensity was larger for the central portion and some western areas of the region, whereas during the year 1982 (Figure 7(c) and 7(d)) the most drought affected areas lay in the northern and western part of the region. Figure 7(e) and 7(f) show that, in general, the western part of the study area exhibited high negative SPI values compared to other parts. This prolonged drought event during the 1980s caused exploding water demand and subsequent impacts in the region, and the eastern Nile basin in general. In the summer of the year 1988, the active storage volume in lake Nasser decreased to less than 20 km^3 (max. capacity 132 km^3) and the water level in Lake Nasser upstream of the Aswan High dam reached a level of 149 m, which was only 2 m above the critical level that would cause damage for the turbines at this time (Afifi 1993; Abdelsalam *et al.* 2008). Figure 8 shows the SAF drought curves that were developed for UBNRB. As it is clear, drought with a short return period (2, 5, 10 and 20 years) and a high degree (SPI ≤ -1.5) cover only small areas of the basin. For instance, droughts of 2- and 5-year return periods with an SPI in the range of –1.5 are expected to cover around 5–20% of the whole region, respectively. This is while droughts with 20- and 50-year return periods can cover 25% and 50% of an area in the same SPI range (–1.5), respectively. Thus, it is clear from Figure 8 that very small parts of the region may be affected by severe droughts (high return periods and/or more negative SPI values). Based on the SAF drought curves shown in Figure 8, if a drought of a 100-year return period dominates around 90% of the whole basin, it will be only a near-normal drought of SPI being greater than –0.6.

CONCLUSION

In this study, a framework of methodologies was presented for the analysis of the temporal and spatial characteristics of the meteorological drought in the upper Blue Nile basin. The SPI was computed at various timescales using spatially distributed precipitation records from 22 meteorological stations. The temporal and spatial

Table 3 | Results of MK test (Bahir Dar station 1960–2008)

SPI time series	SPI 3	SPI 6	SPI 9	SPI 12	SPI 24
h_m	0	0	0	0	0
P value	0.5954	0.9505	0.7478	0.9246	0.1164
Z_{MK}	0.173	0.402	1.127	0.896	0.249
Type of trend	Insignificant	Insignificant	Insignificant	Insignificant	Insignificant

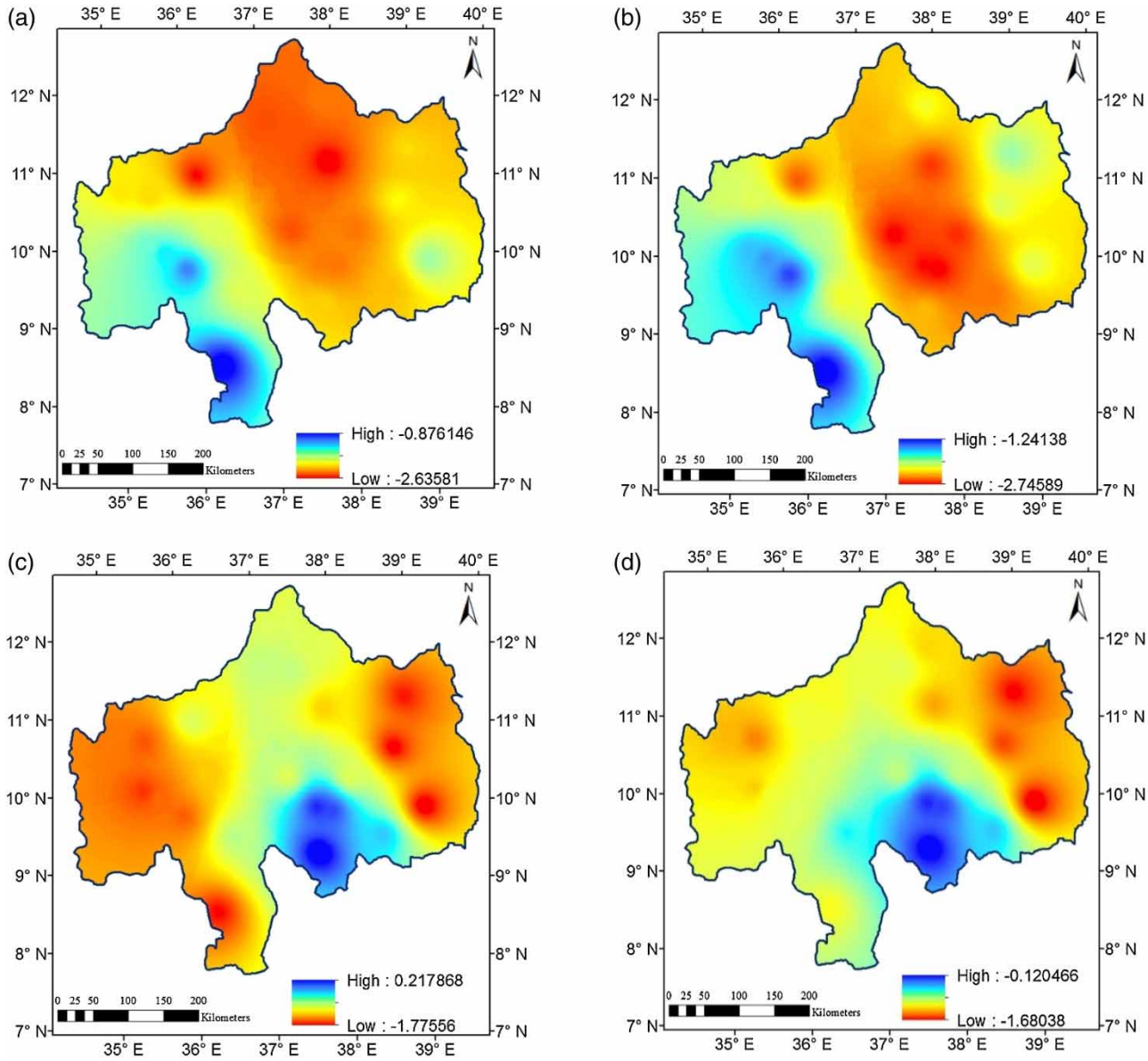

Figure 6 | Spatial extent of some drought events within the study area: (a) SPI3 for June 1965, (b) SPI6 for June 1965, (c) SPI3 for August 1984, (d) SPI6 for August 1984.

drought analyses indicate that the upper Blue Nile Basin received quite frequent moderate to severe droughts with an insignificant trend in the presented SPI series. The region has experienced prolonged and severe droughts during the periods of 1961, 1965 and 1980–1987. In particular, the persistent and prolonged droughts of 1965 and 1982 seriously affected urban water supply and agricultural irrigation. For the 1965 drought, the most affected areas were the area in the center of the UBNRB and with a direction of north to east and southeast, whereas the western and northern areas of UBNRB were mostly affected by the prolonged drought during 1984, which was more severe than the 1965 event. The constructed SAF curves indicated that drought by short return period and high degree cover only small areas of the basin, while only a near-normal drought with a long return period may spread over the whole region. It is hoped that this study will provide useful guidance in

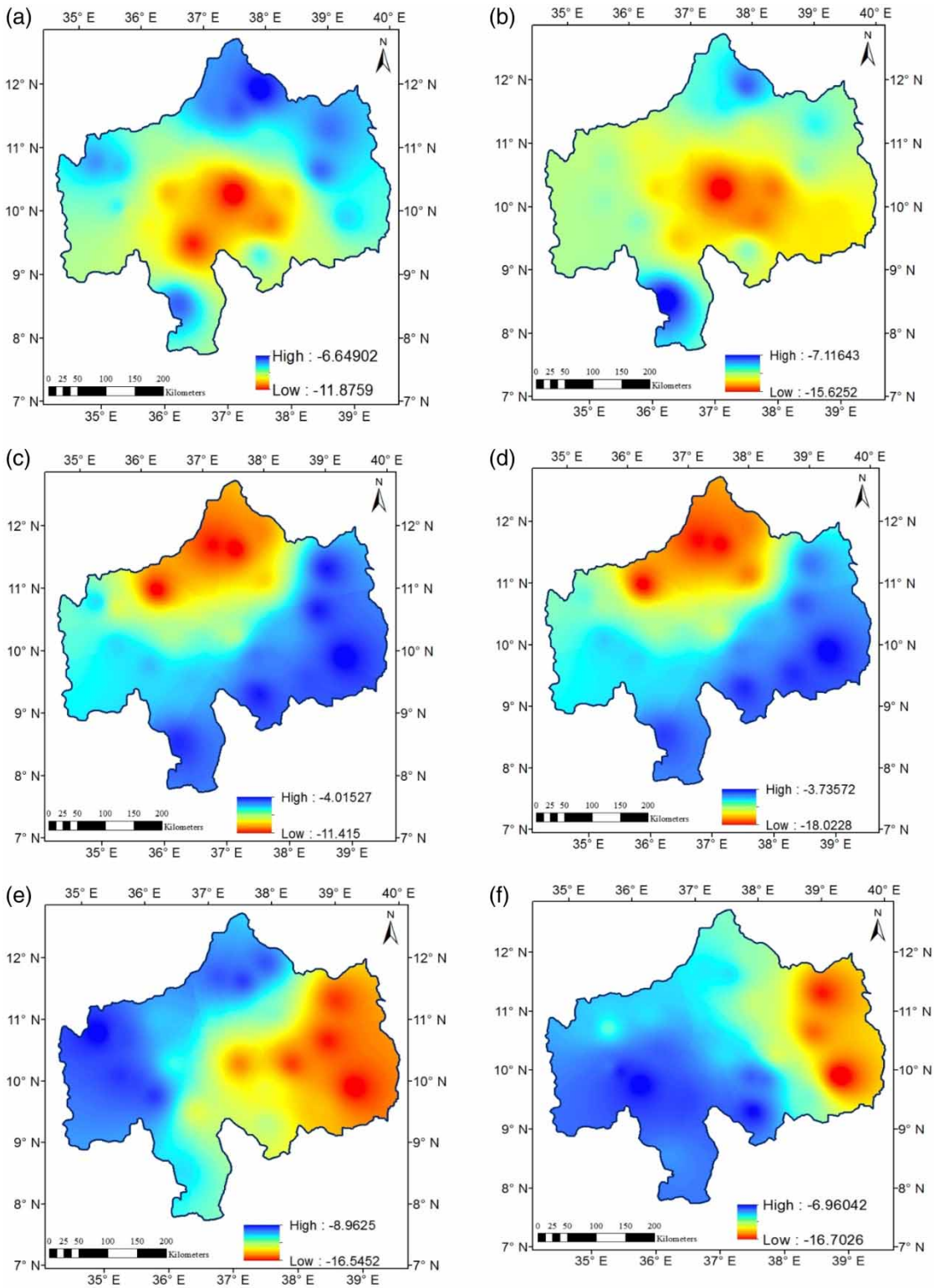

Figure 7 | Spatial distribution of the cumulative annual drought events within the study area: (a) SPI3 for 1965, (b) SPI6 for 1965, (c) SPI3 for 1982, (d) SPI6 for 1982, (e) SPI3 for 1984, (f) SPI6 for 1984.

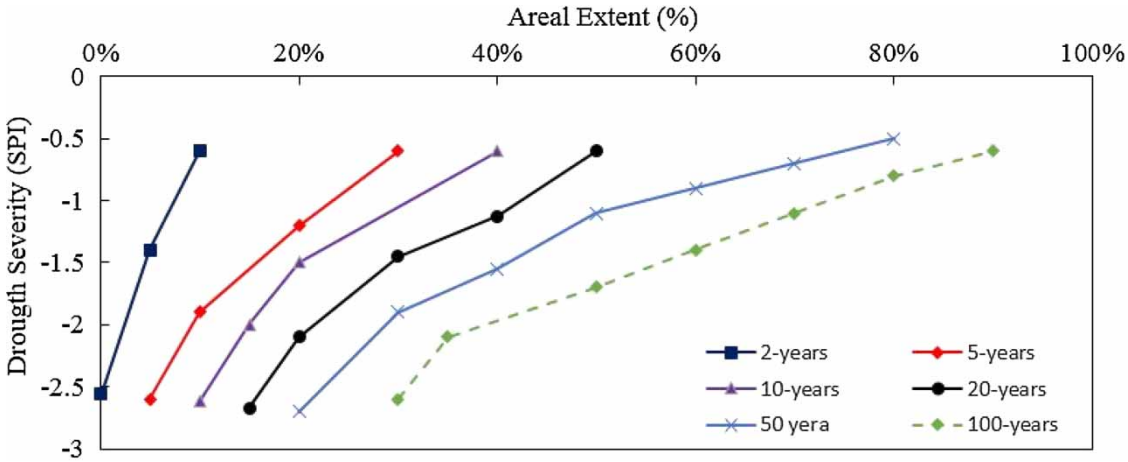

Figure 8 | SAF diagram in the UBNRB.

drought mitigation and adaptation planning in the study area.

ACKNOWLEDGEMENTS

The author thanks the Eastern Nile Technical Regional Office (ENTRO) for kindly providing data which was used for the analysis in this paper.

REFERENCES

Abdelsalam, N. M., Abdelaziz, M. M., Zobaa, A. F. & Aziz, M. S. 2008 Toshka project power operation (Mubarak pump station). In: *12th International Water Technology Conference, IWTC12 2008*, Alexandria, Egypt.

Abu-Zeid, M. A. & Biswas, A. K. 1996 *River Basin Planning and Management*. Oxford University Press, UK.

Afifi, A. B. 1993 Role of Aswan Dam in safeguarding Egypt from floods and droughts. In: *ICOLD 61 Executive Meeting and Symposium*, Cairo, Egypt.

Belayneh, A. 2012 *Short Term and Long Term SPI Drought Forecasts Using Wavelet Neural Networks and Wavelet Support Vector Regression in the Awash River Basin of Ethiopia*. McGill University, Anne de Bellevue, Quebec, Canada.

Blain, G. C. 2012 Monthly values of the standardized precipitation index in the State of São Paulo, Brazil: trends and spectral features under the normality assumption. *Bragantia* **71** (1), 122–131.

Bordi, I. & Sutera, A. 2007 *Drought Monitoring and Forecasting at Large Scale Methods and Tools for Drought Analysis and Management*. Springer, The Netherlands.

Cacciamani, C., Morgillo, A., Marchesi, S. & Pavan, V. M. 2007 *Monitoring and Forecasting Drought on a Regional Scale: Emilia-Romagna Region, 62*. Springer, The Netherlands.

Conway, D. 2000 The climate and hydrology of the upper Blue Nile river. *Geogr. J.* **166** (1), 49–62.

Conway, D. 2005 From headwater tributaries to international river. Observing and adapting to climate variability and change in the Nile Basin. *Glob. Environ. Change* **15**, 99–114.

Dorosh, P. & Rashid, S. 2013 *Food and Agriculture in Ethiopia: Progress and Policy Challenges*. University of Pennsylvania Press, Philadelphia, PA, p. 376.

Dutra, F. D. G., Wetterhall, F. & Pappenberger, F. 2013 Seasonal forecasts of droughts in African basins using the standardized precipitation index. *Hydrol. Earth Syst. Sci.* **17**, 2359–2373.

Edossa, D. C., Babel, M. S. & Gupta, A. D. 2010 Drought analysis on the Awash river basin, Ethiopia. *Water Resour. Manage.* **24**, 1441–1460.

European Commission 2007 *Communication from the Commission to the European Parliament and the Council – Addressing the Challenge of Water Scarcity and Droughts in the European Union*. Commision of the European Communities, Brussels.

Hayes, M. J. 2013 Drought Indices. National Drought Mitigation Center. www.civil.utah.edu/~cv5450/swsi/indices.htm.

IPCC 2012 *Managing the Risks of Extreme Events and Disasters to Advance Climate Change Adaptation: A Special Report of Working Groups I and II of the Intergovernmental Panel on Climate Change*. Cambridge University Press, Cambridge, UK & New York, NY, USA, p. 582.

Karabork, M. C., Kahya, E. & Komuscu, A. U. 2007 Analysis of Turkish precipitation data: homogeneity and the southern oscillation forcings on frequency distributions. *Hydrol. Process.* **21** (23), 3203–3210.

Kendall, M. G. 1975 *Rank Correlation Methods*. 4th edn. Griffin, London.

Keyantash, J. & Dracup, J. 2002 The quantification of drought: an evaluation of drought indices. *Bull. Am. Meteorol. Soc.* **83**, 1167–1180.

Khadr, M. 2011 *Water Resources Management in the Context of Drought: An Application to the Ruhr River Basin in German*. Bericht-Lehr- Und Forschungsgebiet Wasserwirtschaft Und Wasserbau, Wuppertal, Germany.

Khadr, M. 2015 Forecasting of meteorological drought using hidden Markov model (case study: the upper Blue Nile river basin, Ethiopia). *Ain Shams Eng. J.* **7** (1), 47–56.

Khadr, M. & Schlenkhoff, A. 2014 Integration of data-driven modeling and stochastic modeling for multi-purpose reservoir simulation. In: *11th International Conference on Hydroscience & Engineering*, Germany.

Khadr, M. & Schlenkhoff, A. 2014a Mapping of meteorological drought patterns using SPI and different Interpolation methods. In: *11th International Conference on Hydroscience & Engineering*, Germany.

Khadr, M., Gerd, M. & Schlenkhof, A. 2009 Analysis of meteorological drought in the Ruhr Basin by using the standardized precipitation index. In: *International Conference on Sustainable Water Resources Management (SWRM2009)*, Amsterdam, The Netherlands.

Mann, H. B. 1945 Nonparametric tests against trend. *Econometrics* **13**, 245–259.

Masih, I., Maskey, S., Mussá, F. E. F. & Trambauer, P. 2014 A review of droughts on the African continent: a geospatial and long-term perspective. *Hydrol. Earth Syst. Sci.* **18**, 3635–3649.

McKee, T. B., Doesken, N. J. & Kleist, J. 1993 The relationship of drought frequency and duration to time scales. In: *8th Conference of Applied Climatology*, Anaheim, CA.

Mishra, A. K. & Singh, V. P. 2010 A review of drought concepts. *J. Hydrol.* **391** (1–2), 202–216.

NDMC 2006 Defining Drought: Overview. National Drought Mitigation Center. University of Nebraska–Lincoln.

Nour-El-Din, M. M. 2013 Climate change risk management in Egypt: Proposed climate change adaptation strategy for the Ministry of Water Resources & Irrigation in Egypt. UNESCO, Cairo Office, Cairo, Egypt.

Palmer, W. C. 1965 *Meteorological Drought. Research Paper No. 45*. US Weather Bureau, Washington, DC.

Peterson, T. C., Easterling, D. R., Karl, T. R., Groisman, P., Nicholls, N., Plummer, N., Torok, S., Auer, I., Boehm, R., Gullett, D., Vincent, L., Heino, R., Tuomenvirta, H., Mestre, O., Szentimrey, T., Salinger, J., Forland, E. J., Hanssen-Bauer, I., Alexandersson, H., Jones, P. & Parker, D. 1998 Homogeneity adjustments of in situ atmospheric climate data: a review. *Int. J. Climatol.* **18** (13), 1493–1517.

Shafer, B. A. & Dezman, L. E. 1982 Development of a surface water supply index (SWSI) to assess the severity of drought conditions in snowpack runoff areas. In: *Proceedings of the Western Snow Conference*, Fort Collins, CO, pp. 164–175.

Sivakumar, M. V. K., Motha, R. P. & Das, H. P. 2005 *Natural Disasters and Extreme Events in Agriculture*. Springer, Berlin Heidelberg.

Svoboda, M. 2000 An introduction to the drought monitor. *Drought Network News* **12**, 15–20.

Tiwari, K. N., Paul, D. K. & Gontia, N. K. 2007 Characterization of meteorological drought. *J. Hydrol.* **30** (1–2), 15–27.

Valipour, M. 2012 Critical areas of Iran for agriculture water management according to the annual rainfall. *Eur. J. Sci. Res.* **84**, 600–608.

Valipour, M. 2013a Use of surface water supply index to assessing of water resources management in Colorado and Oregon, US. *Adv. Agr. Sci. Eng. Res.* **3**, 631–640.

Valipour, M. 2013b Estimation of surface water supply index using snow water equivalent. *Adv. Agr. Sci. Eng. Res.* **3**, 587–602.

Wilhite, D. A. 2005 *Drought and Water Crises: Science, Technology, and Management Issues*. Taylor & Francis, Boca Raton.

Wilhite, D. A., Sivakumar, M. V. K. & Pulwarty, R. 2014 Managing drought risk in a changing climate: the role of national drought policy. *Weather Clim. Extremes* **3**, 4–13.

WMO (The World Meteorological Organization) 2006 *Impacts of Desertification and Drought and Other Extreme Meteorological Events, no. 1343*. WMO, Geneva, Switzerland.

Woodward, J. C., Macklin, M. G., Krom, M. D. & Williams, M. A. J. 2007 The Nile: evolution, quaternary river environments and material fluxes. In: A. Gupta (ed.), *Large Rivers: Geomorphology and Management*. John Wiley & Sons Ltd, Chichester.

Yue, S., Pilon, P. & Cavadias, G. 2002 Power of the Mann–Kendall and Spearman's Rho tests for detecting monotonic trends in hydrological series. *J. Hydrol.* **259** (1–4), 254–271.

Zaroug, M. A. H., Eltahir, E. A. B. & Giorgi, F. 2014 Droughts and floods over the upper catchment of the Blue Nile and their connections to the timing of El Niño and La Niña events. *Hydrol. Earth Syst. Sci.* **18**, 1239–1249.

First received 26 September 2015; accepted in revised form 25 January 2016. Available online 9 March 2016